Dynamics of the nucleated polymerization model of prion replication

R. Rubenstein [a,*], P.C. Gray [b,*], T.J. Cleland [b], M.S. Piltch [b], W.S. Hlavacek [b,1],
R.M. Roberts [b], J. Ambrosiano [b], J.-I. Kim [c]

[a] *SUNY Down State Medical Center, Brooklyn NY, USA*
[b] *Los Alamos National Laboratory, Los Alamos NM 87545, USA*
[c] *New York State Institute for Basic Research, Staten Island NY, USA*

Abstract

The disease process for transmissible spongiform encephalopathies (TSEs), in one way or another, involves the conversion of a predominantly alpha-helical normal host-coded prion protein (PrP^C) to an abnormally folded (predominantly beta sheet) protease resistant isoform (PrP^{Sc}). Several alternative mechanisms have been proposed for this auto-catalytic process. Here the dynamical behavior of one of these models, the nucleated polymerization model, is studied by Monte Carlo discrete-event simulation of the explicit conversion reactions. These simulations demonstrate the characteristic dynamical behavior of this model for prion replication. Using estimates for the reaction rates and concentrations, time courses are estimated for concentration of PrP^{Sc}, PrP^{Sc} aggregates, and PrP^C as well as size distributions for the aggregates. The implications of these dynamics on protein misfolding cyclic amplification (PMCA) is discussed.
© 2006 Elsevier B.V. All rights reserved.

Keywords: Nucleated polymerization; Model system; Prion replication; TSE; PrP aggregation; Protein misfolding cyclic amplification (PMCA)

1. Introduction

Transmissible spongiform encephalopathies (TSE) are fatal, infectious, neurodegenerative diseases. Examples of TSEs include: bovine spongiform encephalopathy (BSE) in cattle, scrapie in sheep, chronic wasting disease in deer and elk, and Creutzfeldt–Jakob disease (CJD), Gerstmann–Straussler–Scheinker syndrome (GSS), and fatal familial insomnia (FFI) in humans. The unconventional infectious agents, termed prions, are highly resistant to inactivation and are responsible for disease transmission. Prions consist primarily of a misfolded protein designated PrP^{Sc}. There are several theories concerning replication of the infectious agent. One theory is termed the prion hypothesis and suggests the infectious agent is protein only with the complete absence of an agent-specific nucleic acid. According to the prion hypothesis, the agent replicates by inducing a host-coded glycoprotein (designated PrP^C) to undergo a conformational change to form new PrP^{Sc} molecules in a self-propagating process [1–4]. This self replication occurs only in the presence of PrP^C [5]. The mechanism by which PrP^C is converted into PrP^{Sc}, and the subsequent formation of amyloid, is uncertain. Several models have been proposed to explain the self-replication of the protein-only infectious agent [3]. The nucleation-dependent aggregation mechanism, or nucleated polymerization model, suggests that aggregates of PrP^{Sc} propagate by assimilating PrP^C monomers into a growing structure. Thus, the aggregate becomes the infectious unit, with conversion being synonymous with integration of PrP^C into the aggregate. Another model is the cooperative autocatalysis model. According to this, a mixed aggregate of PrP^{Sc} and PrP^C converts to an aggregate of PrP^{Sc} by allosteric interactions. A third model, the heterodimer mechanism, is also based on the conformational change of PrP^C into PrP^{Sc} ($PrP^C + PrP^{Sc} \rightarrow PrP^{Sc} * PrP^C \rightarrow 2PrP^{Sc}$) but does not require any prior aggregate

---

* Corresponding authors. Gray is to be contacted at Los Alamos National Laboratory, MS F-603, Los Alamos, NM 87545 USA. Tel.: +1 505 665 0812; fax: +1 505 606 1504. Rubenstein, SUNY Downstate Medical Center, Department of Biochemistry, 450 Clarkson Avenue, Brooklyn, NY 11203 USA. Tel.: +1 718 270 2019; fax: +1 718 270 2459.

E-mail addresses: richard.rubenstein@downstate.edu (R. Rubenstein), pcgray@lanl.gov (P.C. Gray).

[1] Center for Nonlinear Studies, Los Alamos National Laboratory, Los Alamos NM 87545, USA.

formation. The original model for the disease was based on this hypothesis, the autocatalytic conformational change of PrP^C to PrP^{Sc}. By this model, a resulting exponential run-away of the formation of PrP^{Sc} would be limited in its end stage only by the production rate of PrP^C. While it is possible to construct models of this kind that could account for the rarity of the occurrence of the disease, as well as the time course presented, their sensitivity and potential instability to small variation in the reaction rates makes their applicability to biological systems questionable [3].

In this paper, we explore the dynamical behavior of the nucleated polymerization model of Masel et al. [6] using Monte Carlo discrete-event simulation. The dynamics of this model were explored by Nowak et al. [7], using a method based on ordinary differential equations (ODEs), and semi-quantitative results were discussed. This work was extended to a cellular model for the overall spread of the disease through a two-dimensional tissue model. Our goal in simulating the dynamics of this model is to gauge whether the underlying reasoning, given current parameter estimates, is sufficient to explain the known pathology of the disease. Also, we are interested in quantitative estimates of experimentally measurable quantities and the implications of these quantities for the design of protein misfolding cyclic amplification (PMCA) protocols (see below). Knowledge of the dynamics can give insight into critical features of the model and suggest experimental tests with the potential to validate or invalidate the model as a candidate for prion replication.

2. The nucleated polymerization model (NPM) for prion replication

The nucleated polymerization model [6] was proposed to explain the self-replication process. Masel and co-workers cast
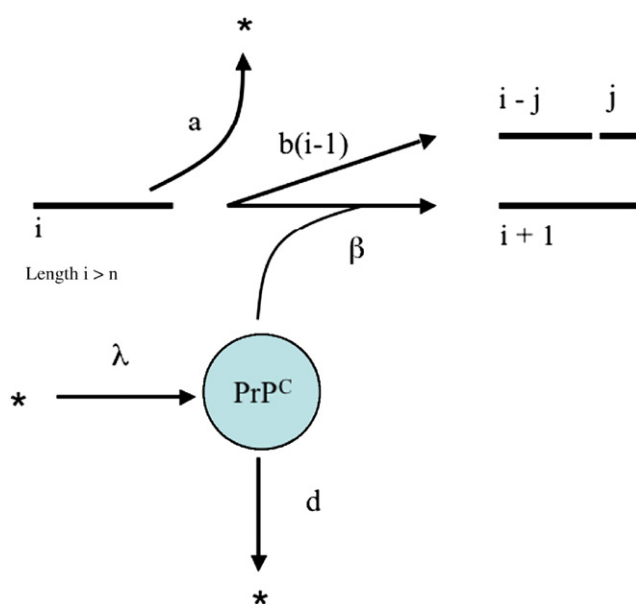

Fig. 1. Diagramatic representation of nucleated polymerization model for prion replication (after Masel et al. [6]), '*' denotes production from metabolic pathways, or elimination by degradation or sequestration (as indicated by arrows).

the model as a set of ODEs and explored the relative influence of the kinetic parameters, on overall predictions of the model. Fig. 1 is a schematic of the three main model components. The first is the normal metabolic production and degradation of PrP^C with rate coefficients λ and d respectively. The second is a competitive process between elongation of the linear aggregates and cleavage of the aggregates, with rates β and b respectively. Finally, there is degradation and/or sequestration of the aggregates (e.g. through condensation) with rate coefficient a. This last component lumps any process which reduces the "infectivity" of the aggregates into a single process. The model posits that conversion may occur at either end of a linear aggregate of PrP^{Sc} for aggregates of sufficient length. Aggregates below this threshold length, n, are unstable to rapid degradation. Aggregates are equally likely to cleave at any site along the linear aggregate (thus the $b(i-1)$ term for probability of cleavage of an aggregate of length i). The parameters of the model used in this study are derived from Masel et al. [6] with the exception of n, the minimum chain length. In a later paper by Masel et al. [8], it was argued that a prion must be a smaller polymer than previously thought with the minimum chain length n being 2 or 3, and mean chain length s being between 4 and 15. Here we assume $n=3$.
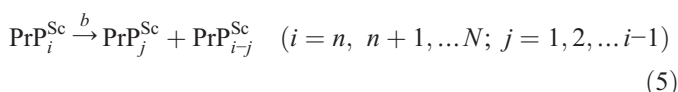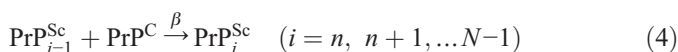
3. Numerical methods

We solved the kinetics of the proposed biochemical network using the stochastic reaction method of Gillespie [9]. Our implementation includes numerical efficiency improvements introduced by Gibson and Bruck [10]. The software that implements the method is an open-source C++ program called *BioReactor* [11]. In addition to this, results were compared against results from the model as implemented in *BioNetGen* [12,13]. Both of these tools were also used for simulations based on ODEs, which were solved by using the software package CVODE [14].

A brief description of Gillespie's [9] stochastic reaction method follows. Given the list of all the chemical reactions in a network, the method advances the system one reaction event at a time. As reaction events fire, reactants are stoichiometrically decremented and products are incremented. The likelihood that a reaction will fire is rigorously determined from the probability distributions based on the reaction rate, reaction order (uni-molecular, bimolecular, etc.) and the quantity of each reactant. For each reaction in the network, a "next firing time" is determined by randomly sampling from its probability distribution. Increasing the number of reactant particles for a given reaction, and/or the reaction rate, increases the likelihood that it will fire. The reaction with the earliest sampled firing time is always chosen as the next reaction. Once this reaction fires, the system time and the affected species quantities are updated. In this way, the system advances through time.

This brute-force stochastic method is best used in cases where one or more of the chemical species is present in small quantities (or it is suspected that quantities may become small). This technique gives an exact solution of the chemical master equation [9,15], and will by nature include important statistical

fluctuations. The method can be used to obtain ensemble-averaged values. Alternatively, it can be used to examine individual realizations of systems dynamics.

For this investigation, the nucleated polymerization model proposed by Masel et al. [6] was simulated. This model includes the following reactions:

$$* \xrightarrow{\lambda} PrP^C \tag{1}$$

$$PrP^C \xrightarrow{d} * \tag{2}$$

$$PrP_i^{Sc} \xrightarrow{a} * \tag{3}$$

$$PrP_{i-1}^{Sc} + PrP^C \xrightarrow{\beta} PrP_i^{Sc} \quad (i = n, \ n+1, ... N-1) \tag{4}$$

$$PrP_i^{Sc} \xrightarrow{b} PrP_j^{Sc} + PrP_{i-j}^{Sc} \quad (i = n, \ n+1, ... N; \ j = 1, 2, ... i-1) \tag{5}$$

$$PrP_2^{Sc} \xrightarrow{\gamma} 2PrP^C \tag{6}$$

The rate coefficients for these reactions are defined in the previous section, and N is the maximum polymer chain length included in the simulation ($N=25$ or 50). It should be noted that PrP_1 is equivalent to PrP^C, since it is assumed that PrP^{Sc} is unstable and rapidly degrades. Reaction (6) represents the rapid breakdown of aggregates at or below n at rate γ, which we set to a large number ($\gamma = 100$). For a given value of N, reactions (1)–(6) represent $N(N+3)/2 - 3$ reactions. However, due to symmetry considerations (e.g., $PrP_5^{Sc} \xrightarrow{b} PrP_2^{Sc} + PrP_3^{Sc}$ and $PrP_5^{Sc} \xrightarrow{b} PrP_3^{Sc} + PrP_2^{Sc}$ can be presented as one reaction with rate $2b$) the number of reactions represented by reactions (1)–(6) can be reduced to ($N(N+8))/4 - 3$ for even N or $(N(N+8)-1)/4 - 3$ for odd N. In our simulation, we've chosen $N=40$ which made for 477 reactions after invoking symmetry.

The values of the rate constants were taken from Masel et al. [6,8] and converted to appropriate units (in the cases where a range of values were given, the average value of the range was used): $a=0.047/\text{day}$, $b=0.0314/\text{day}$, $\beta=0.00292/\text{day}$, $\lambda=2400/\text{day}$, $d=4/\text{day}$, and $X_0 = \lambda/d = 600$, where X_0 is the initial, steady state, concentration of PrP^C. These values, along with a nominal assumed volume based on the volume of a single neuronal cell, are given in Table 1.

Table 1
Estimates of model parameters used in Monte Carlo simulation of nucleated polymerization model for prion replication

Parameter	Estimate
a	0.047 per day
β	$2.92 \ 10^{-3}$ per day
b	0.0314 per day
λ	1800 to 3000 (2400 per day)
d	3 to 5 (4 per day)
$x_0 \ (\lambda/d)$	600
n	2 to 3
Volume	10^{-12} l

4. Simulation results

To demonstrate the dynamical behavior of the NPM, we have performed a set of simulations independently varying (1) the degradation rate of aggregates, (2) the competition between aggregate elongation and cleavage, and (3) the production rate of PrP^C. The initial conditions for these simulations include an assumption that a typical steady state concentration of PrP^C is nano-molar. This leads to a few hundred molecules per cell. Since there is no source term for aggregates of PrP^{Sc}, the system is seeded with a few aggregates (typically 3 to 30) at the minimum aggregate size ($i=3$). Typical estimates for the concentration of free PrP^{Sc} are cited as being in the femto-molar range. At this concentration, the process we are modeling represents events occurring for one cell in a thousand or fewer.

In Figs. 2, 3 and 4 we have plotted the time histories of PrP^C concentration, the concentration of total PrP^{Sc}, the concentration of PrP^{Sc} aggregates, and the mean chain length of the aggregates for the three studies we performed. The first of these shows the impact of the polymerization process on the concentration of the normal protein, which was initially set at its equilibrium level (i.e. $[PrP^C] = X_0 = \lambda/d$). The total PrP^{Sc} and aggregate concentrations represent what would be seen by assaying protein and infectivity respectively. The ratio of PrP^{Sc} molecules to the aggregate concentration is essentially the mean chain length.

5. Aggregate degradation

The aggregation rate was adjusted by varying the assumed value of the parameter a in the model while holding the other parameters fixed. Fig. 2 shows the time histories for simulations varying the degradation rate of PrP^{Sc} aggregates ($a=0.0235$, 0.047, 0.094 per day). The variation in the rate constant a is less than an order of magnitude. Nevertheless, as a peaks this is sufficient to choke off the elongation process, as can be seen from the constant PrP^C concentration (upper left frame), and the absence of increased PrP^{Sc} (upper right/lower left frame). Beyond this, the variation of a appears only to affect the final concentration of PrP^{Sc}, which can be seen by the similarity in shape of the growth curves for PrP^{Sc} concentration in the other two cases.

6. Elongation vs. cleavage of aggregates

The effect of competition between aggregate elongation and cleavage was studied by varying the ratio b/β. Fig. 3 shows the time courses for variation of the ratio b/β, the ratio of the rate of cleavage to the rate of elongation ($b/\beta=0.5$, 1.0, 2.0, 10.0, 20.0, 30.0, 40.0). These ratios were achieved by maintaining the value for b and varying the value for β. All other parameters were held constant. The effect of this ratio on the model is to attenuate the formation of aggregates, and the time to onset of their accumulation. For the largest values of this ratio (30.0 and 40.0) the process is completely shut off. We have included the case with $b/\beta=30.0$ (in all but the plots for mean chain length) to highlight this. The major effect of these parameters is to foreshorten or lengthen the onset of PrP^{Sc} saturation.

7. PrP^C production

The effect on the model of PrP^C production was studied by varying λ. Fig. 4 shows the time courses for variation of the production rate of PrP^C ($\lambda = 1200$ to 2400 per day). The only apparent effect of the PrP^C production rate is to affect the final saturation level of PrP^{Sc}.

8. Size distributions of aggregates

An expression for the steady state value for the mean chain length of aggregates can be obtained from the differential equations for the model. Following Masel et al. [6], let the concentration of normal protein be denoted as x, the aggregates as y (with y_i denoting the concentration of aggregates of length i) and z the concentration of PrP^{Sc} molecules (i.e. $z = \sum_i i y_i$), and s denote the mean chain length of the aggregates (i.e. $s = z/y$.) Then from the equation for the aggregates, (see Appendix A of Masel et al. [6] for details) one obtains a steady state expression for s, $s = a/b + 2n - 1$. Fig. 5 shows the steady state distributions for various choices of a/b (recall $n = 3$). The amplitude decreases as a/b increases, because we are holding a fixed value for b ($b = 0.0314$) and increasing a. However, as can be seen from the bottom frame, which shows the mean chain length for these simulations as a function of a/b, they are in good agreement with the derived

expression. These simulations were run out to a final time of 1 year. The distributions shown are averaged over times greater than 200 days, a time when all cases have reached approximate steady state. This tendency toward steady state can be seen from the time histories of mean chain length in Figs. 2, 3 and 4 (with the exception of those cases where the process was shut down). The initial development of the distribution starts with generation of aggregates of much larger mean chain length. This is because of the initial tendency for elongation over breakage of the seed aggregates (see below). Fig. 6 demonstrates that the parameters a and b can be adjusted to achieve larger steady state values for s, at the expense of the time required to reach steady state. Shown are two cases; one in which we have used the canonical value of $b = 0.0314$ and set $a/b = 1$ yielding $s = 6$, and a second in which we have scaled b by a factor of 0.05 and set $a/b = 8$ yielding $s = 13$. For the example shown, we have included reactions up to aggregates of 50 in length, to accommodate the increased value of s. As can be seen, as a/b is increased, to obtain similar concentration of aggregates a must be scaled back or aggregates are degraded so rapidly that the reaction eventually cannot be maintained. The cost of this is that the time to achieve a steady state condition, as indicated by the time history in Fig. 6, becomes unreasonably long (greater than a year for $a/b = 8.0$.) An alternative to scaling a/b, which yields this shift to larger values of s, is to scale up the production level, λ, of the normal protein. However, we have
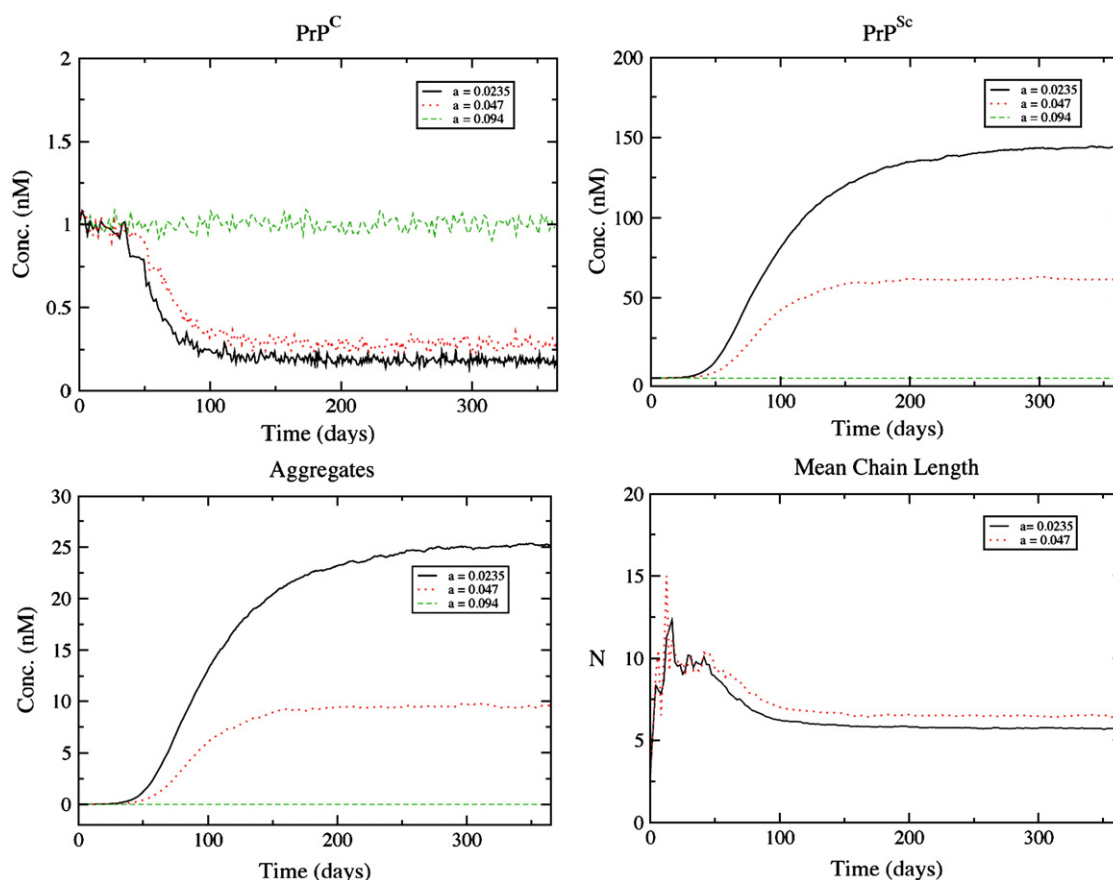

Fig. 2. Time histories of prion replication with variation in degradation/elimination of aggregates, parameter 'a' [$a = 0.0235, 0.047, 0.094$ per day], in nucleated polymerization model, shown are; PrP^C concentration (top left), total PrP^{Sc} Concentration (top right), PrP^{Sc} aggregates (bottom left), and mean chain length (bottom right).

found that any significant shift requires a production level much higher than the nominal value for λ.

9. Implication for protein misfolding cyclic amplification (PMCA)

The dynamics of the NPM model have interesting implications for development of *in vitro* assays. There has been an ongoing effort to exploit the PrP conversion process to develop assays with similar amplification to the polymerase chain reaction (PCR). This method, protein misfolding cyclic amplification (PMCA) [16], seeks to reproduce *in vitro* the TSE disease process on an accelerated time scale. In this technique an exogenous source of normal protein, such as brain homogenate, is added to an unknown sample suspected of containing PrP^{Sc}. The mixture is incubated for a time then sonicated to re-suspend and break up aggregates. Finally, fresh PrP^{C} is added to complete a cycle. The protocol for this technique attempts to maintain gross excess of PrP^{C} at all times. This would be optimal for a direct conversion process for PrP, however the situation is a little different if the process is similar to the NPM model. As mentioned above, the initial phase of the NPM model has the mean chain length going to larger size than mean size for the final size distribution of aggregates. Why this is so can easily be seen by comparing the propensities for a reaction

in which a chain is broken and one in which it elongates, $P_b = b(z - y) = by(s - 1)$ and $P_e = \beta xy$, respectively. Here we denote PrP^{C} as x, PrP^{Sc} as z and PrP^{Sc} aggregates of mean length s as y, as above. Since initially $\beta X_0 \gg b(s - 1)$, the seed PrP^{Sc} aggregates are more likely to undergo elongation than breakage. This is true until the total number of breakage sites offsets the relative size of b to β, as well as compensating for the concentration of normal protein. At this point the propensities are equal yielding an expression for s:

$$s = \frac{\beta}{b}x + 1$$

When this condition is satisfied the size distribution of aggregates will relax to its final shape as the rate of breakage overtakes the elongation rate. If, as in the protocols for PMCA, the initial concentration of the normal protein, X_0, is set sufficiently high that the conversion process during one cycle has little affect on it, the seed aggregates will grow to large values of s before significant cleavage occurs. Thus the conversion kinetics will look closer to linear growth than exponential growth, since the number of conversion sites is nearly constant. This suggests that, if the conversion process is NPM or a similar polymerization process, the optimal conversion rate would be achieved by maintaining conditions that minimize s, or
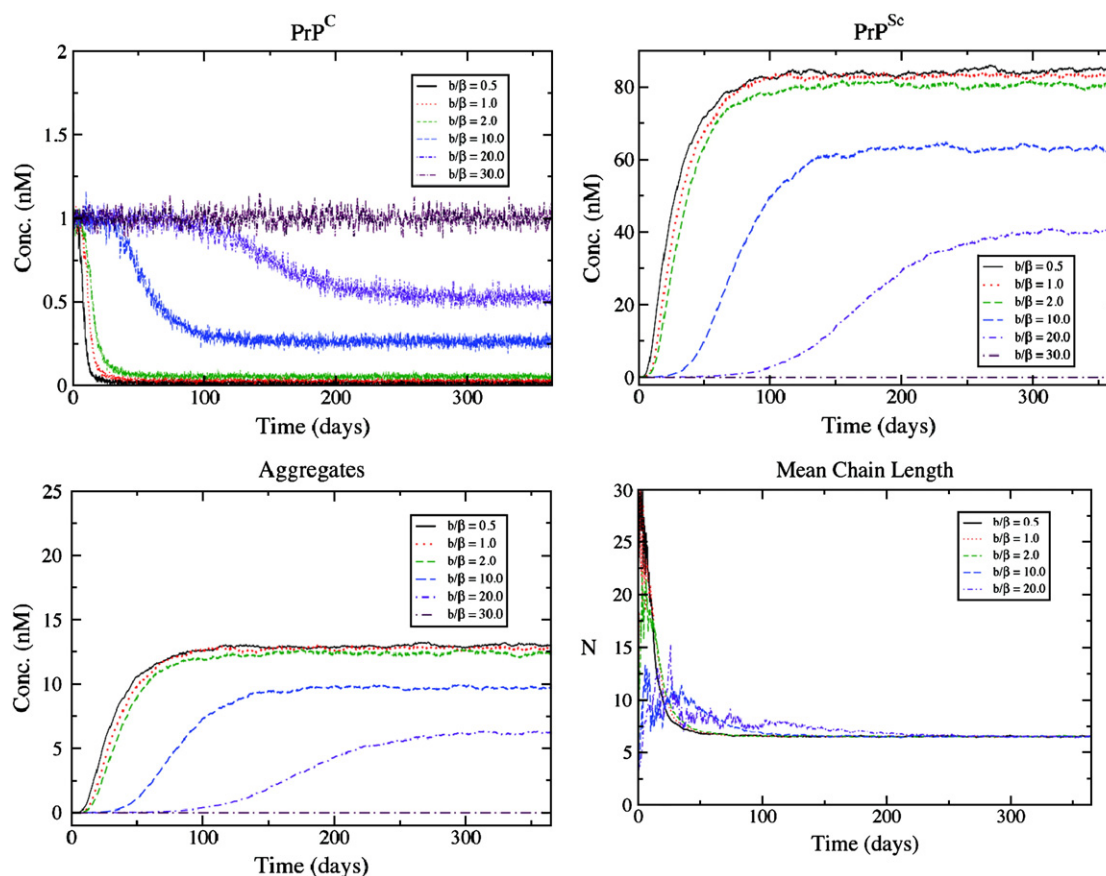

Fig. 3. Time histories of prion replication with variation in ratio of chain elongation to chain breakage, ratio 'b/β' [b/β=0.5, 1.0, 2.0, 10.0, 20.0, 30.0, 40.0], in nucleated polymerization model, shown are; PrP^{C} concentration (top left), total PrP^{Sc} Concentration (top right), PrP^{Sc} aggregates (bottom left), and mean chain length (bottom right).
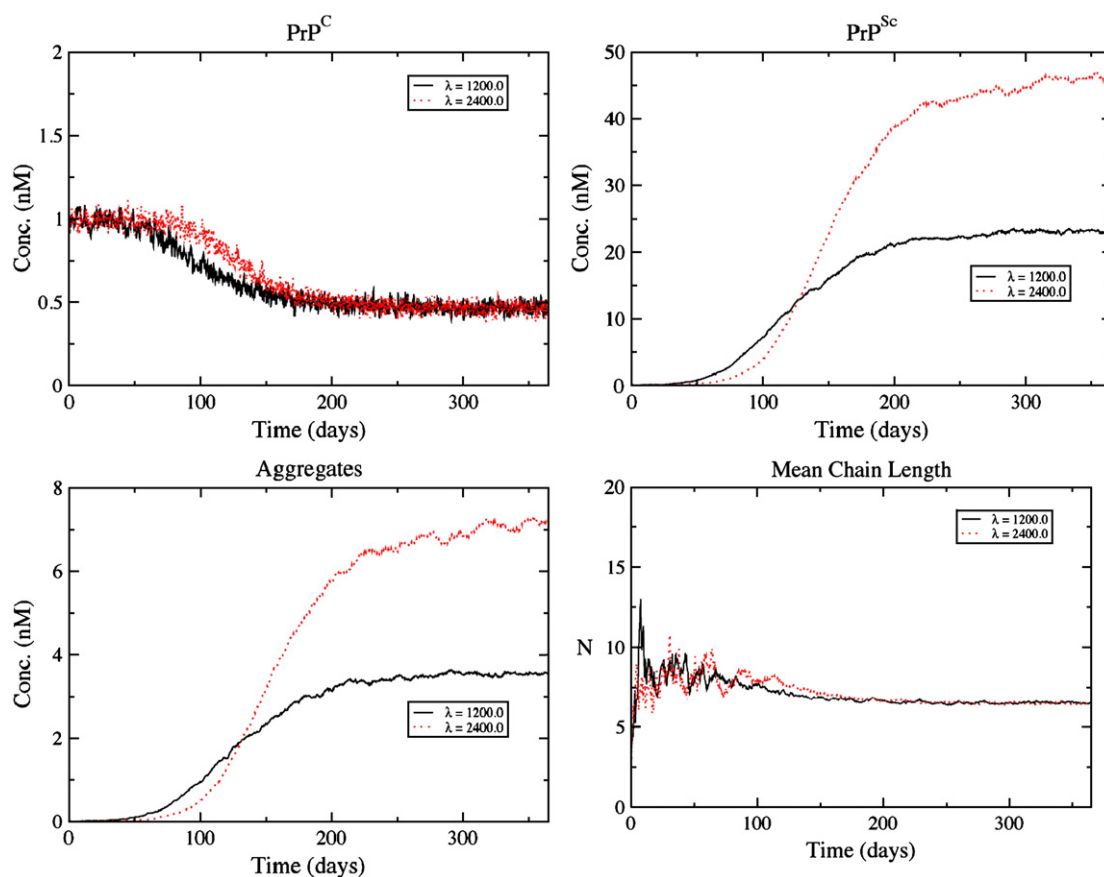
Fig. 4. Time histories of prion replication with variation in PrP^C production, parameter 'λ' [$\lambda = 1200, 2400$ per day], in nucleated polymerization model, shown are; PrP^C concentration (top left), total PrP^{Sc} Concentration (top right), PrP^{Sc} aggregates (bottom left), and mean chain length (bottom right).

maximize y. This might be achieved by supplying the exogenous PrP^C continually at much lower concentrations than used in the bolus associated with a PMCA cycle.

10. Discussion

This simulation study effectively demonstrates the essential dynamical features of the Nucleated Polymerization Model. Competition among the three basic processes allows for considerable expressiveness in the behavior of the model. The results presented above are qualitatively consistent with those demonstrated by Nowak et al. [7], in which the model was simulated using ordinary differential equations. The saturation level of PrP^{Sc} appears to be determined by a combination of all three processes: production/destruction of PrP^C, elongation/ cleavage of aggregates, and sequestration/destruction of aggregates. The time to saturation appears to be a function of the competition between elongation, balanced by degradation, and cleavage of the aggregates. It is interesting that over moderate variation of the current estimates for the model parameters, there is little variation in the resultant size distribution of aggregates. Large shifts in the distribution can be achieved by varying the essential parameters by orders of magnitude, however this results in a requirement for a large rate of production of the normal protein or an extremely long time for the system to reach steady state. If the latter is the case then it suggests that

understanding dynamics, during which the mean chain length is longer, might be more important for understanding the TSE disease process than the steady state conditions.

The simulations presented here assumed that the normal protein was initially at a concentration consistent with equilibrium levels calculated from nominal metabolic rates. Given this assumption, the effect of the polymerization mechanism is to drop PrP^C concentration to a new equilibrium level consistent with the addition of a sink term due to the conversion of the normal protein to the abnormal from. This new level is given approximately by $X_f = \lambda/(d+\beta)$. This expression is approximate because there is a small additional source-term, which reflects the cleavage of small sections of the aggregates that revert to PrP^C. This source term is dependent on the size distribution of aggregates and is therefore not constant. Another question that arises from these effects, is to what extent the loss of the normal protein is compensated by changes in metabolic rates or rates of expression. As constructed, if the initial equilibrium level of PrP^C is maintained through increased expression, the model will revert to an attenuated exponential growth of PrP^{Sc}. In this case, the kinetics are similar to the direct conversion model, with final growth rate limited by the expression level of the normal protein.

The most striking feature we find from this study is the relative insensitivity of the final aggregate size distribution to moderate variation of current estimated parameters. Any significant shift in the distribution requires changes in the parameters
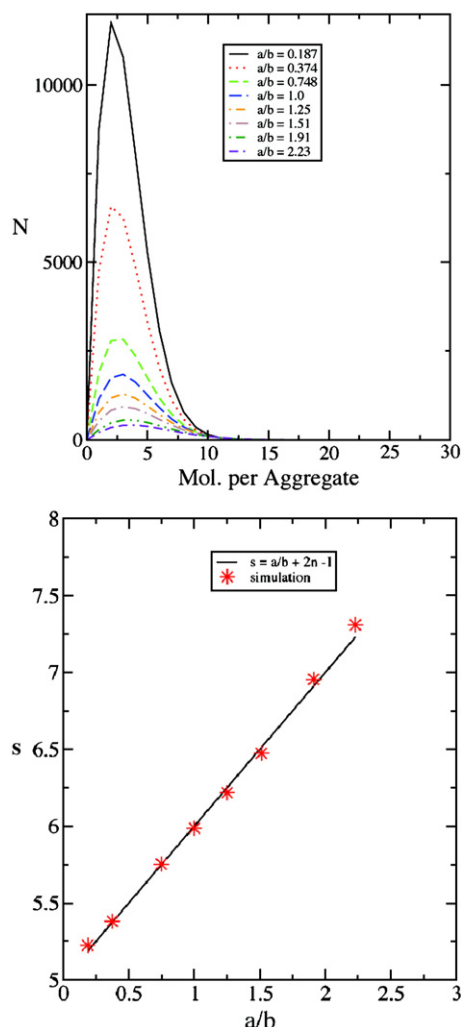
Fig. 5. Final size distributions of aggregates (top) as a function of the ratio a/b (rate of degradation of aggregates to cleavage rate) value of 'b' is fixed at $b=0.314$ and 'a' is varied, comparison of steady state main aggregate length 's' as a function of 'a/b' and derived expression for 's' at steady state (bottom).

so large (an order of magnitude in scale) that the time required to establish a steady state aggregate size distribution becomes unreasonably long in comparison to the duration of the disease (much greater than a year). Even in such cases, the tendency is to initially generate longer chains of aggregates which are then cleaved to generate a distribution with much smaller mean length (similar to that seen in the time histories of mean chain length in Fig. 6). This suggests that a good way to check the validity of the model would be to develop a method for estimating the mean size of the infectious agent. The NPM postulates that the infectious unit is an aggregate, and that each aggregate has two active sites at either end of the linear chain. Thus, as the aggregates grow, the ratio of active sites to protein drops, and with it the infectivity of the PrP^{Sc}. By this reasoning, the time history of mean chain length represents the history of infectivity of the disease agent during the development of the disease. The final mean chain length, as seen in the distributions in Fig. 5, is the scale factor between the infectious aggregates and the total PrP^{Sc}. This suggests that an end point assay for the

mean chain length might be appropriate for validating the model. A way of determining this experimentally would be to assay a preparation for both total PrP^{Sc} and infectivity in order to obtain the scale factor. There are, of course, difficulties with this. First, because of the sticky nature of PrP^{Sc}, macroscopic aggregates which form during purification might be expected to dominate over the "normal" aggregation process. Similarly, re-suspension of the protein during the purification protocol might alter the mean chain length by mechanically inducing cleavage.

Besides these suggestions for experimental validation of the model, we have examined the effect of the dynamics associated with the model on PMCA. The PMCA protocol has an underlying assumption that the kinetics of the conversion process are those of direct conversion. The optimal conditions for direct conversion and polymerization models, such as NPM, are sufficiently different that the PMCA might constitute a good experimental validation of the models in and of itself. A
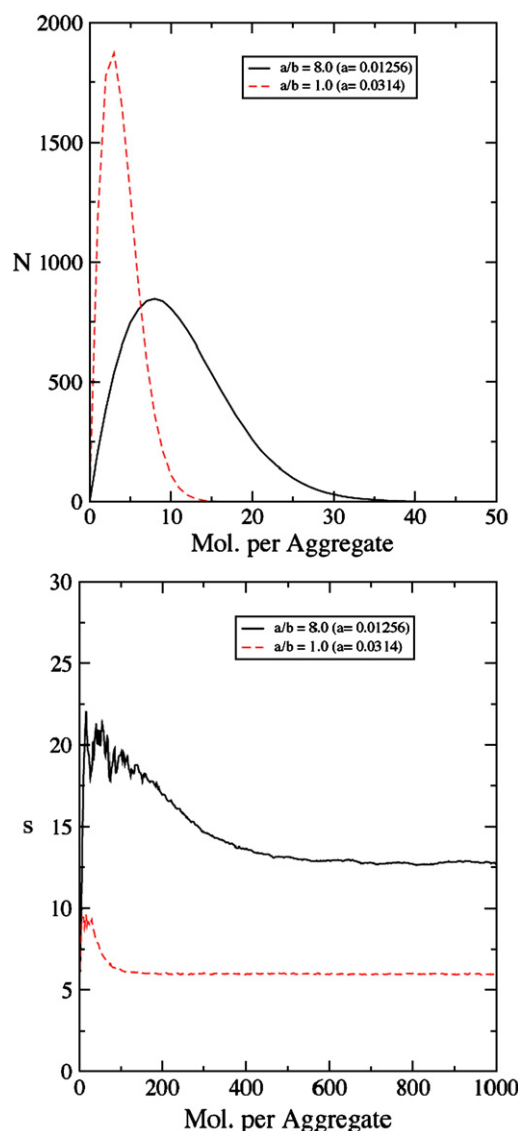

Fig. 6. Shift of final value of 's', and overall shape of size distribution of aggregates, with scaled choices of 'a' and 'b' (top), and time history of 's' (bottom).

comparison of PMCA performance, total PrP^{Sc} produced, by modification of the protocol would be an interesting approach to examine the underlying kinetics, and lead to improvements in diagnostic techniques.

Finally it should be remembered that the methods used in these studies do not include any effects expected from spatial dependence. There is also good reason to believe that a critical component of the TSE disease process involves some form of active transport of the agent [17]. The inclusion of transport and spatial variation in the model at the level of an individual cell, and the appropriate numerical approach to studying it, should be subjects for future investigation.

Acknowledgements

References

[1] F.E. Cohen, K.M. Pan, Z. Huang, M. Baldwin, R.J. Fletterick, S.B. Prusiner, Structural clues of prion replication, Science 264 (1994) 530.

[2] P.T. Landsbury, Mechanism of scrapie replication, Science 265 (1994) 1510.

[3] M. Eigen, Prionics or the kinetic basis of prion diseases, Biophys. Chem. 63 (1996) A1–A18.

[4] C. Weissmann, Molecular genetics of transmissible spongiform encephalopathies, J. Biol. Chem. 274 (1) (1999) 3–6.

[5] H. Bueler, A. Aguzzi, A. Sailer, R.A. Greiner, P. Autenried, N. Aguet, C. Weissmann, Mice devoid of prp are resistant to scrapie, Cell 73 (1993) 1339.

[6] J. Masel, V.A.A. Jansen, M.A. Nowak, Quantifying the parameters of prion replication, Biophys. Chem. 77 (1999) 139–152.

[7] M.A. Nowak, D.C. Krakaur, A. Klug, R.M. May, Prion infection dynamics, Integr. Biol. 1 (1998) 3–15.

[8] J. Masel, N. Genoud, A. Aguzzi, Efficient inhibition of prion replication by PrP-Fc$_2$, J. Mol. Biol. 345 (2005) 1243–1251.

[9] D.T. Gillespie, A general method for numerically simulating the stochastic time evolution of coupled chemical reactions, J. Comp. Phys. 22 (1976) 403–434.

[10] M.A. Gibson, J. Bruck, Efficient exact stochastic simulation of chemical systems with many species and many channels, J. Phys. Chem., A 104 (2000) 1876–1889.

[11] R.M. Roberts, T.J. Cleland, P.C. Gray, J.J. Ambrosiano, Hidden Markov model for competitive binding and chain elongation, J. Phys. Chem., B 108 (20) (2004) 6228–6232.

[12] M.L. Blinov, J.R. Faeder, B. Goldstein, W.S. Hlavacek, BioNetGen: software for rule-based modeling of signal transduction based on the interactions of molecular domains, Bioinformatics 20 (2004) 3289–3291.

[13] J.R. Faeder, M.L. Blinov, B. Goldstein, W.S. Hlavacek, Rule-based modeling of biochemical networks, Complexity 10 (2005) 22–41.

[14] S.D. Cohen, A.C. Hindmarsh, CVODE users guide, LLNL Report UCRL-MA-118618, October 1994.

[15] D.T. Gillespie, A rigorous derivation of the chemical master equation, Physica, A 188 (1992) 404–425.

[16] G.P. Saborio, B. Permanne, C. Soto, Sensitive detection of pathological prion protein by cyclic amplification of protein misfolding, Nature 411 (2001) 810–813.

[17] N.A. Mabbott, M.E. Bruce, The immunobiology of TSE diseases, J. Gen. Virol. 82 (2001) 2307–2318.